Homogeneous nanocables from double-walled boron-nitride nanotubes using first-principles calculations

Zhuhua Zhang,[1,2] Xiao Cheng Zeng,[2] and Wanlin Guo[1,*]
[1]*Institute of Nano Science, Nanjing University of Aeronautics and Astronautics, Nanjing 210016, China*
[2]*Department of Chemistry and Nebraska Center for Materials and Nanoscience, University of Nebraska–Lincoln, Lincoln, Nebraska 68588, USA*

(Received 23 April 2010; revised manuscript received 3 June 2010; published 12 July 2010)

Since electrons injected to a homogenous wire always tend to concentrate on its surface, heterogeneous coaxial structures are generally necessary to make nanocables with an insulating sheath. Here we reveal from first-principles calculations that double-walled boron-nitride nanotubes could be natural homogeneous nanocables as injected electrons prefer abnormally to concentrate on the inner semiconducting tube while the outer tube remains insulating. The ratio of extra electrons on the inner tube to total carriers in the double-walled nanotubes can be tuned widely by changing either the tube diameter or the local tube curvature through radial deformation, both attributed to the predominant band filling and weak enhancement in Coulomb interaction within the inner wall where the sublattice asymmetry is strongly attenuated by curvature effect. This exotic charge screening is universal for any form of electron-doping sources.

DOI: 10.1103/PhysRevB.82.035412 PACS number(s): 61.46.Fg, 21.10.Ft, 61.72.U−, 71.15.Mb

I. INTRODUCTION

Electric charges introduced to a single-phase material tend to gather on its surface due to electrostatic effect. This effect becomes particularly strong in low-dimensional nanostructures such as nanowires[1] and nanotubes.[2] However, for nanoelectronic applications, it is important to confine the charge carriers to the interior of the nanomaterial protected by an insulating layer. A common approach to realizing this confinement is to manufacture heterogeneous coaxial structures with a functional core and an insulating sheath,[3] known as nanocables as they are akin to the conventional cables used for electricity transmission. In the past decade, various heterogeneous nanocable structures were reported and all could be sorted into two types based on the core-shell interactions. The first type is heterostructured coaxial nanowires with a semiconducting or metallic core and an insulating crystalline sheath.[3–11] Nanocables of this type typically entail complex interfacial geometry between the core and sheath due to strong core-sheath interaction, which are likely to induce trap states detrimental to carrier transport. The second type is the hybrid nanotubes with the inner core to be a semiconductor tube or metal wire and the outer tube (sheath) being insulating.[12–16] The core and sheath interact through relatively weak van der Waals interaction. Nevertheless, manufacturing the second type of nanocables still requires delicate fabrication processes which render the demand for mass production impractical.

All single-walled boron nitride nanotubes (BNNTs) with diameter larger than 9.5 Å possess a constant insulating band gap (~5.8 eV), independent of their morphology.[17–19] On the other hand, single-walled BNNTs with diameter less than 9.5 Å exhibit strong dependence of band gap on their chirality and diameters. Especially, the band gap of a zigzag BNNT decreases rapidly with increasing tube curvature.[20,21] For example, the band gap goes down to 3.1 eV when the diameter is 3.35 Å.[20] Due to high thermal stability of B-N bonding, thin BNNTs show higher stability than the carbon nanotubes (CNTs) of the same diameter.[22] In experiments, thin BNNTs often exist in multiwalled forms, with a predicted average interwall spacing of 3.35 Å,[23,24] similar to recently synthesized 3-Å-diameter (2,2) CNT inside a multiwalled CNT.[25] Hence, in diametrically relatively small double-walled BNNTs (DBNNTs) with diameter less than 16 Å, there exist large energy band offsets between the inner and outer tubes, which may drive abnormal charge carrier distribution and thus open an exciting possibility for homogeneous nanocables. Still, whether the conductive carriers can naturally gather in the interior of such homogenous systems remains unknown. Here, we show by first-principles calculations that injected extra electrons in DBNNTs prefer to concentrate on the inner tube while the outer tube is insulating, giving rise to functional homogenous nanocables. Moreover, the carrier concentration on the inner tube can be widely tuned by changing the tube curvature, thereby providing tailored functional nanocables for nanoelectronics applications. It is more important that the demonstrated conception of homogenous nanocable is not limited to BNNTs only, but turns out to be a generic feature for a wide family of inorganic double-walled tubular structures.

II. MODELS AND METHODS

The calculations are performed within the framework of density-functional theory as implemented in Vienna *ab initio* simulation package.[26] Ultrasoft pseudopotentials for the atomic core and the local density approximation (LDA) for the exchange-correlation potential are adopted. Test calculations using generalized gradient approximation give almost the same results. A kinetic-energy cutoff of 435 eV is used in the plane-wave expansion. We focus on the DBNNTs with zigzag configurations because of the preference of zigzag orientation during the growth of BNNTs.[27] We model injected electrons to the DBNNTs by adjusting the charge neutrality level with a uniformly positive jellium countercharge. Dipole correction[28] to the total energy (less than

10^{-3} meV/atom) is neglected due to relatively low levels of charge injection considered in this study. The supercell consists of two primitive tube cells along the tube axis with nearest nanotubes separated by a vacuum region of 10 Å. The change in average electron intercalation energy is less than 0.01 meV/atom when four primitive tube cells are included in the supercell. The Brillouin-zone integration is sampled by up to 20 special k points and all atomic positions and lattice constants are optimized by using the conjugate gradient method until the maximum force on each atom is less than 0.01 eV/Å.

III. RESULTS AND DISCUSSIONS

To evaluate the quality of DBNNT nanocables, we calculate the ratio of extra electrons on the inner tube (n_{inner}) to the total electrons injected to the DBNNTs (n_{total}). We then compare this ratio with the ideal nanocable model which consists of a CNT core and a BNNT sheath. Figure 1(a) shows the ratio n_{inner}/n_{total} as a function of charge-injection level. For the (5,0)@(13,0) DBNNT, the ratio n_{inner}/n_{total} can be over 80% when the charge-injection level is less than 0.012 electrons/atom, even higher than that of the ideal nanocable of (5,0) CNT enclosed in a (14,0) BNNT. The charge-injection level of 0.012 electrons/atom corresponds to a carrier concentration of 1.4×10^{21} e/cm^3, a desirable value for electric transport, which can be realized by applied bias voltages or electrochemical doping. The ratio n_{inner}/n_{total} is somewhat reduced at higher charge-injection level but is still over 55% when the charge-injection level is up to 0.02 electrons/atom. Moreover, the ratio n_{inner}/n_{total} can be further significantly enhanced by reducing tube diameter of the DBNNT, especially at higher charge-injection level. For DBNNTs with smaller diameter than (5,0)@(13,0), surprisingly, the ratio n_{inner}/n_{total} is higher than that of the ideal nanocable over the entire range of charge-injection levels. The high ratio n_{inner}/n_{total} is robust to the change in the interwall spacing as well as the presence of Stone-Wales defects in the tube walls. Such high ratio n_{inner}/n_{total}, combining with the predicted high stability of these DBNNTs,[24] promises great potential of DBNNTs as homogenous functional nanocables.

To understand this unexpected charge-distribution phenomenon, first, we examine electronic band filling of DBNNTs by charge injection. Figure 1(c) shows the band structures for the (5,0)@(13,0) DBNNT at different charge-injection levels. Without charge injection, the conduction-band minimum and valence-band maximum are due to the inner and outer tubes [Fig. 1(c), left], respectively, well consistent with previous calculations.[23] When extra electrons are introduced into the DBNNT, the conduction band from π^* states of the inner tube is filled first and all the inner-tube bands undergo a rigid upshift with respect to the outer-tube bands so that the valence band maximum of the system is also due to the inner tube, once the charge-injection level is over 0.0035 electrons/atom [red solid lines in Fig. 1(c)]. This band character indicates that electron-injected DBNNT is a natural coaxial element, of which the inner wall is an n-doped semiconductor while the outer wall remains insulating. This is further illustrated by the charge redistribution at charge-injection level of 0.007 electrons/atom as shown in Fig. 1(b), where the accumulated electrons are highly concentrated on the inner tube. Interestingly, we also observe two regions with depleted electron density around the concave side of both the tube walls, forming two dipole layers normal to the tube walls to minimize the system energy. However, there are some differences in the region of high charge-injection levels. When the charge-injection level is raised to 0.014 electrons/atom, the nearly free electron (NFE) states[29] downshift, and start to cut E_F [blue lines with triangles in Fig. 1(c)] due to a universal electrostatic mechanism,[30] which gradually shifts the NFE states from inside to outside of the DBNNT. Therefore, above this charge-injection level, part of extra electrons will distribute outside the tube to fill the NFE states, which, combining with the growing electrostatic effect, leads to a rapid decrease in n_{inner}/n_{total}. The critical charge-injection level for lowering the NFE states to cut E_F increases monotonically with decreasing tube diameter, ranging from 0.011 electrons/atom for the (8,0)@(16,0) DBNNT to 0.019 electrons/atom for the (4,0)@(11,0) DBNNT, because the NFE states in thinner BNNTs locate at higher energy levels due to stronger NFE-π^* hybridization.[24]

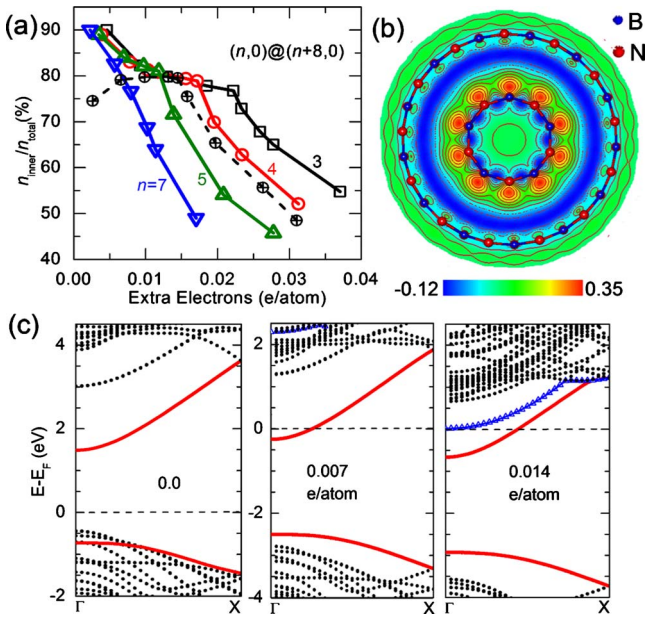

FIG. 1. (Color online) Distribution of injected electrons in DBNNTs with different diameters. (a) Ratio n_{inner}/n_{total} for the $(n,0)@(n+8,0)$ DBNNTs $(n=3-7)$ as a function of charge-injection level. Black dash line is for an idea case of a (5,0) CNT sheathed in a (14,0) BNNT. (b) Charge redistribution of the injected electrons in the (5,0)@(13,0) DBNNT at the charge-injection level of 0.007 electrons/atom. The solid lines represent the isosurface of charge accumulation while the dash lines represent the isosurface of charge depletion. The isosurface spacing is set to 1.0×10^{-3} e/Å^3. (c) Band structures for the (5,0)@(13,0) DBNNT at charge-injection levels of 0.0, 0.007, and 0.014 electrons/atom (left to right). The highest valence band and the lowest conduction band due to the inner tube are marked by red solid lines. The nearly free electron states are denoted by blue line of triangles.

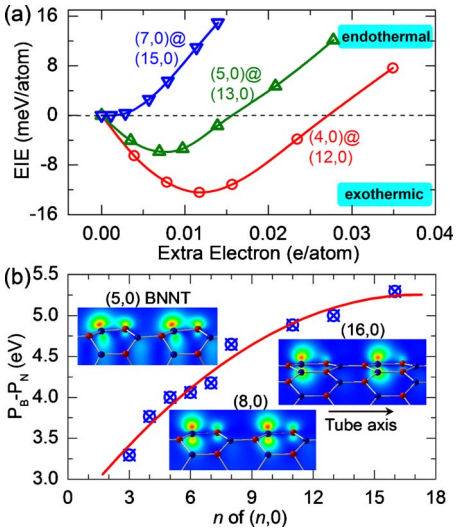

FIG. 2. (Color online) Mechanism for the preference of injected electrons on the inner tube of DBNNTs. (a) EIE of $(n,0)@(n+8,0)$ DBNNTs as a function of the charge-injection level. (b) Difference between average core potentials at B and N atoms as a function of BNNT size. The three insets display slices of charge densities of the unoccupied states within an energy interval of 2 eV above the conduction band minimum, for the (5,0), (8,0), and (16,0) BNNTs, respectively. Red (gray), yellow (white), green (light gray), and blue (dark) colors represent the magnitude of the charge density in descending order.

The predominant filling of inner-tube bands, however, can only qualitatively explain the variation in n_{inner}/n_{total} but cannot account for its high value because similar band filling of inner wall can be realized in some double-walled CNTs (DCNTs) as well, such as the (5,0)@(14,0) DCNT, where the n_{inner}/n_{total} is significantly lower than the values presented here.[2,31,32] To have a better understanding of the high ratio value of n_{inner}/n_{total}, we also examine the electron intercalation energy (EIE) in DBNNTs. The EIE for a DBNNT is calculated by $\mathrm{EIE}=E_C-E_0$, where E_C and E_0 represent the total energies of the charged and uncharged DBNNTs, respectively. We treat the double-walled system as a two-layer cylindrical capacitor so that the EIE for a DBNNT can be expressed as $\mathrm{EIE}_D=\mathrm{EIE}_i(n_{inner})+\mathrm{EIE}_o(n_{outer})+An_{inner}^2$, where $\mathrm{EIE}_i(n_{inner})$ and $\mathrm{EIE}_o(n_{outer})$ represent the EIE for the inner and outer tubes, respectively, and the An_{inner}^2 term represents the electrostatic energy with A being a positive constant for a given DBNNT. Figure 2(a) shows that the EIE_D is positive (endothermic), and increases monotonically with increasing the charge-injection level for a normal-sized (7,0)@(15,0) DBNNT due to largely enhanced Coulomb interaction when injected electrons distribute exclusively on B atoms of polar B-N bonds. In contrast, for thinner DBNNTs, the EIE_D decreases first toward a negative minimum value and then increases as the charge-injection level increases; and the EIE_D decreases rapidly with decreasing tube diameter at a given charge-injection level. These results indicate that with thinner DBNNTs, the charge-injection process is energetically more favorable as it becomes exothermic over a wider range of charge-injection levels. To gain a deeper insight, we examine the electrostatic potentials at the B and N atoms for each tube wall. We find that the electrostatic potential difference between the B and N atoms decreases quadratically with increasing the tube curvature [see Fig. 2(b)], mainly due to the reduced potential at B atoms. As a result, the *empty* π^* states, which are contributed mostly by the B atoms in a normal (16,0) BNNT, are now partially contributed by the N atoms with decreasing the tube diameter, particularly in thinner BNNTs [see insets of Fig. 2(b)]. Meanwhile, the potential inside the tube is also significantly lowered as the tube becomes thinner, leading to partial transfer of the *empty* π^* state to the outside of the tube and the formation of surface dipole, normal to the tube wall.

Actually, the EIE for a single-walled BNNT is mainly contributed by the energy gain due to electron filling of the empty conduction band states and the energy loss due to the enhanced Coulomb interaction between injected electrons on the tube wall. When injected electrons fill the π^* states of the inner tube of thin DBNNTs, the enhancement in Coulomb interaction is largely offset by the intersite π^* state transfer and associated surface dipole, resulting in a large energy gain, namely, negative $\mathrm{EIE}_i(n_{inner})$; whereas the Coulomb interaction remains significantly strong when the π^* states of the outer tube are filled as there is no such significant state transfer. Therefore, the $\mathrm{EIE}_i(n_{inner})$ can be more negative in thinner DBNNTs and is able to offset the positive $\mathrm{EIE}_o(n_{outer})$ as well as electrostatic energy to make EIE_D negative. Consequently, at relatively low charge-injection levels, the extra electrons in thin DBNNTs tend to gather on the inner tube to minimize the system energy, owing to the reduced Coulomb energy. This phenomenon is absent in DCNTs, where the two sublattices are completely symmetrical regardless of the tube curvature so that both the $\mathrm{EIE}_i(n_{inner})$ and $\mathrm{EIE}_o(n_{outer})$ are negative and weakly diameter-dependent, and the electrostatic effect leads to their low ratio n_{inner}/n_{total}.[31] In fact, electronic property of DCNTs is very sensitive to the interwall distance because of their relatively small band gap due to the high sublattice symmetry.[33] This behavior is less pronounced in DBNNTs because all BNNTs have relatively large band gap.[24] Inspired by the mechanism involving the sublattice asymmetry, we also consider other composite nanotubes, such as recently synthesized SiC nanotubes,[34] and find that this abnormal screening behavior is a generic feature in these composite nanotubes.

In view of the strong diameter dependence, we expect that modulating tube curvature through radial deformation can further enhance the ratio n_{inner}/n_{total} in large DBNNTs. The latter would be desirable for applications as larger DBNNTs can be more easily manufactured. As nanotubes are extremely flexible to distortions along radial direction, the radial deformation of DBNNTs is experimentally very feasible and has been widely used to design versatile functional nanodevices.[35–38] As such, we first squash a normal-sized (8,0)@(16,0) DBNNT along the y direction as shown in the inset of Fig. 3, and the strain in the y direction is defined as $\varepsilon_y=(D-D_y)/D$, where D is the diameter of the undeformed DBNNT and D_y is the minor axes of the deformed tube. The structure is fully relaxed at each given ε_y except for the atoms at the squashed sites, which are fixed at preset positions. Figure 3 shows the ratio n_{inner}/n_{total} as a function of

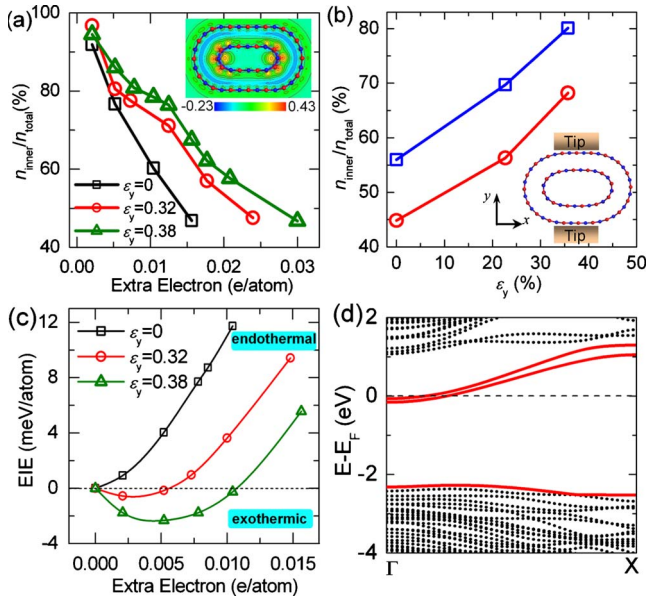

FIG. 3. (Color online) (a) Ratio n_{inner}/n_{total} for the (8,0)@(16,0) DBNNT under various radial strains in the y direction: ε_y=0 (squares), 0.32 (circles), and 0.38 (triangles) as a function of the charge-injection level. Inset: the charge redistribution induced by introducing 0.007 electrons/atom in the squashed (8,0)@(16,0) DBNNT with ε_y=0.32; the solid lines represent the isosurface of charge accumulation while the dash lines represent the isosurface of charge depletion. (b) Ratio n_{inner}/n_{total} for the (12,0)@(20,0) DBNNT as a function of radial strain ε_y at charge-injection levels of 0.008 (blue squares) and 0.012 electrons/atom (red circles). The inset shows the axial view of the DBNNT deformation. (c) EIE of the (8,0)@(16,0) DBNNTs under different radial strain ε_y as a function of the charge-injection level. (d) Band structure of the squashed (8,0)@(16,0) DBNNT with ε_y=0.38 and at an charge-injection level of 0.0073 electrons/atom. The highest valence band and the lowest conduction band due to the inner tube are marked by red solid lines.

charge-injection level at different ε_y. As expected, the ratio n_{inner}/n_{total} is considerably enhanced with increasing ε_y for the (8,0)@(16,0) DBNNT at all charge-injection levels considered. The injected electron carriers are mainly transferred to the two high curvature regions of the inner tube [see inset of Fig. 3(a)]. At a high charge-injection level of 0.015 electrons/atom, the ratio n_{inner}/n_{total} of the deformed DBNNT is up to 65% at ε_y=0.32, comparable to the case of the (5,0) CNT inside (14,0) BNNT. In addition, the EIE can change from endothermic in the undeformed case to exothermic at ε_y=0.32 when the charge-injection level is less than 0.006 electrons/atom, as shown in Fig. 3(c). Further increasing ε_y can lead to higher ratio n_{inner}/n_{total} and lower EIE. In the band structure for the squashed (8,0)@(16,0) DBNNT at ε_y=0.38 and charge-injection level of 0.07 electrons/atom, both the valence band maximum and conduction band minimum are from the inner tube [Fig. 3(d)], suggesting that the charged system could act as a homogenous nanocable. At ε_y=0.38, the band gap of the inner tube is reduced to 2.1 eV (LDA value) while the gap of the outer tube is still up to 3.89 eV, large enough for insulating purpose. To make our results more general, we have also squashed the (12,0)@(20,0)

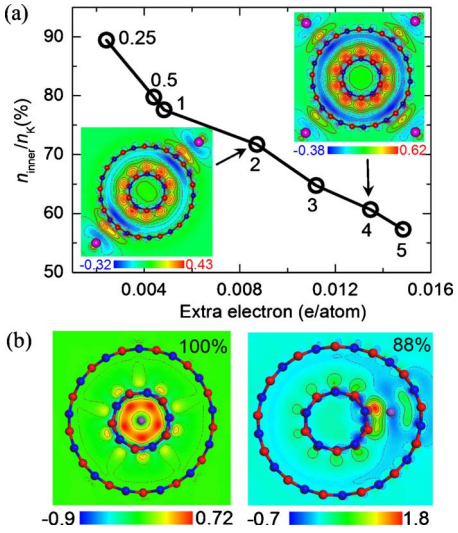

FIG. 4. (Color online) (a) Ratio n_{inner}/n_K in the (5,0)@(13,0) DBNNT as a function of charge-injection level from potassium (K) atoms. Insets show the charge redistribution induced by doping two and four K atoms per supercell. The number at each point denotes the amount of K atoms per tube cell. (b) The charge redistribution induced by doping a Li atom per tube cell at different locations with respect to the (5,0)@(13,0) DBNNTs, where the values at the top right corner denote the ratio n_{inner}/n_{Li}. The solid lines represent the isosurface of charge accumulation while the dash lines represent the isosurface of charge depletion The isosurface spacing is set to 0.8 $\times 10^{-3}$ e/Å^3. The pink balls denote K (Li) atoms.

DBNNT with a tube diameter up to 15.6 Å. It is shown that the ratio n_{inner}/n_{total} is still greatly increased with increasing ε_y at different charge-injection levels, see Fig. 3(b). Especially, at charge-injection level up to 0.012 electrons/atom (the supercell now contains 256 atoms), the ratio n_{inner}/n_{total} can be raised to 69% at ε_y=0.36. Clearly, large DBNNTs can be used as homogenous nanocables under nanomechanical loading.

From the strain energy of the DBNNTs induced by radial deformation, we can roughly estimate the pressures involved in the radial strains. Assuming that forces act on the flat areas of tube along the radial direction, the involved pressure is estimated to be about 12.1 GPa at ε_y=0.32 for the (8,0)@(16,0) DBNNT, and it is greatly reduced to 4.8 GPa at ε_y=0.36 for the (12,0)@(20,0) DBNNT. These pressures are very feasible in experiments considering that the pressure from the tip of an atomic force microscopy can easily reach up to tens of gigapascals. Also, it is important that all these radial strains are still in elastic range and the deformed nanotubes can resume spontaneously to their original perfect shapes when the pressures are released. Therefore, the demonstrated mechanical modulation of carrier distribution is potentially reversible.

Our conclusions are quite universal for any form of *n*-type charge-doping sources with the countercharges in an accessible location away from the tube wall, such as alkali atoms and other charge-transfer cationic dopants. To confirm this point, we perform similar calculations for the potassium-adsorbed (5,0)@(13,0) DBNNT, as shown in Fig. 4(a). It is found that the ratio of n_{inner}/n_K (n_K denotes transferred elec-

trons from potassium atoms) changes with charge-injection level similarly to that shown in Fig. 1(a). In particular, the ratio n_{inner}/n_K can be up to 70% at a charge-injection level of 0.01 electrons/atom, even though the potassium atoms are adsorbed on the outer tube. One may note that the ratio n_{inner}/n_K is somewhat reduced from that in the doped DBNNTs with jellium countercharge. The reason is mainly due to the difference in the spatial distribution of the positive countercharges. The NFE states are more sensitive to K doping, and cross the Fermi level at a lower charge-injection level than in the case of jellium model. As a result, the NFE states are retreated to the outside of the nanotube at an extremely low charge-injection level, and therefore the ratio of electron accumulation on the inner wall is lower than those shown in Fig. 1(a) over the entire range of charge-injection levels. However, the absolute values of ratio n_{inner}/n_K are still comparable to the case of CNT enclosed within a BNNT. Small Li atoms located within the inner tube or in the inter-wall region give higher ratio of extra electrons on the inner tube, see Fig. 4(b).

We also examine the hole-injected DBNNTs but find an extremely low ratio n_{inner}/n_{total} of holes (about 1%). Injecting holes into the DBNNTs can greatly raise the system total energy regardless of the tube diameter and carrier concentration. This is because the curvature effect can hardly change the distribution of the occupied π states due to weak π-σ hybridization in zigzag BNNTs, that is, no appreciable transfer of the π states either from the N to B sites or from tube inside to outside. So the π states are dominantly contributed by N atoms for both the inner and outer tube walls. As a result, the Coulomb interaction between injected hole carrier cannot be alleviated in both the tube walls and the holes tend to distribute on the outer wall to minimize the electrostatic energy. Finally, we note a recent experiment presenting a field-induced inside-out failure in multiwalled BNNTs,[39] in stark contrast to the electrically driven outside-in thinning of multiwalled CNTs.[40,41] This experiment, to some extent, corroborates our results here although the experimental sizes of BNNTs are larger than our calculated ones.

IV. CONCLUSIONS

In summary, we have demonstrated by first-principles calculations that DBNNTs can become promising functional homogenous nanocables. When extra electrons are introduced to the DBNNT, higher curvature in the inner tube causes more significant intersite transfer of the unoccupied states and thus greatly alleviates the coulomb interaction among the electron carriers on this tube wall. This makes the inner tube as a potential well surrounded by higher potential of the outer tube, which leads to the preference for electron carriers to reside on the inner tube as schematically illustrated in Fig. 5. The ratio of electron carriers on the inner tube to total carriers in the DBNNT can be significantly enhanced by decreasing the tube diameter or increasing local curvature through radial deformation and it can even surpass the ratio for heterogeneous tubular nanocables. This abnormal screening behavior in DBNNTs is expected to be a generic feature for a group of composite double-walled tubular structures. Therefore, the conception of functional homogeneous nanocables is viable as an essential feature at the nanoscale and can be exploited in creating nanoelectronic devices and circuits.

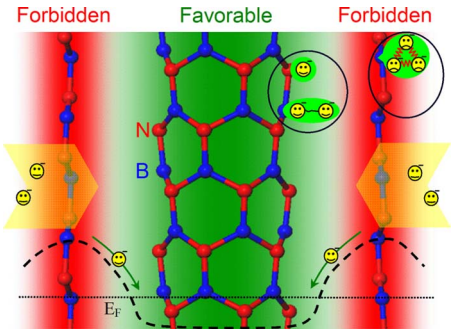

FIG. 5. (Color online) Schematic illustration of mechanism for the preference of injected electrons to reside on the inner wall of the (5,0)@(13,0) DBNNT. The fresh green regions (around the inner wall) illustrate the empty states to be occupied by the injected electrons. The regions around the outer wall are forbidden for electron occupation. The head balls illustrate only the relative amount of charge. The dash line illustrates the potential profile across the DBNNT for injected electrons.

ACKNOWLEDGMENTS

W.G. is supported by the 973 Program (Grant No. 2007CB936204), National NSF (Grant No. 10732040), and Jiangsu Province NSF (Grant No. BK2008042) of China. X.C.Z. is supported by U.S. Office of Naval Research (Grant No. N00014-05-1-0432) and the Nebraska Research Initiative, and by the University of Nebraska Holland Computing Center. Z.Z. is supported by the Jiangsu Province Scientific Research Innovation Project for Graduate Students (Grant No. CX07B-064z).

*wlguo@nuaa.edu.cn

[1] F. Kassubek, C. A. Stafford, and H. Grabert, Phys. Rev. B **59**, 7560 (1999).

[2] G. Chen, S. Bandow, E. R. Margine, C. Nisoli, A. N. Kolmogorov, V. H. Crespi, R. Gupta, G. U. Sumanasekera, S. Iijima, and P. C. Eklund, Phys. Rev. Lett. **90**, 257403 (2003).

[3] A. M. Morales and C. M. Lieber, Science **279**, 208 (1998).

[4] L. Fu, Y. Liu, Z. Liu, B. Han, L. Cao, D. Wei, G. Yu, and D. Zhu, Adv. Mater. **18**, 181 (2006).

[5] J. A. Goebl, R. W. Black, J. Puthussery, J. Giblin, T. H. Kosel, and M. Kuno, J. Am. Chem. Soc. **130**, 14822 (2008).

[6] X. L. Fu, Y. J. Ma, P. G. Li, L. M. Chen, and W. H. Tang, Appl.

Phys. Lett. **86**, 143102 (2005).
[7] S. Guo, J. Li, W. Ren, D. Wen, S. Dong, and E. Wang, Chem. Mater. **21**, 2247 (2009).
[8] J. H. He, Y. Y. Zhang, J. Liu, D. Moore, G. Bao, and Z. L. Wang, J. Phys. Chem. C **111**, 12152 (2007).
[9] H. Zhang, C. Wang, and L. Wang, Nano Lett. **2**, 941 (2002).
[10] Y. Zhang, K. Suenaga, C. Colliex, and S. Iijima, Science **281**, 973 (1998).
[11] J. Terao, S. Tsuda, Y. Tanaka, K. Okoshi, T. Fujihara, Y. Tsuji, and N. Kambe, J. Am. Chem. Soc. **131**, 16004 (2009).
[12] Y. Zhu, Y. Bando, D. Xue, F. Xu, and D. Golberg, J. Am. Chem. Soc. **125**, 14226 (2003).
[13] K. Suenaga, C. Colliex, N. Demoncy, A. Loiseau, H. Pascard, and F. Willaime, Science **278**, 653 (1997).
[14] W. Mickelson, S. Aloni, W. Q. Han, J. Cumings, and A. Zettl, Science **300**, 467 (2003).
[15] Z. Zhang, W. Guo, and G. Tai, Appl. Phys. Lett. **90**, 133103 (2007).
[16] W. Han, P. Redlich, F. Ernst, and M. Ruhle, Appl. Phys. Lett. **75**, 1875 (1999).
[17] A. Rubio, J. L. Corkill, and M. L. Cohen, Phys. Rev. B **49**, 5081 (1994).
[18] N. G. Chopra, R. J. Luyken, and K. Cherrey, Science **269**, 966 (1995).
[19] X. Blase, A. Rubio, S. G. Louie, and M. L. Cohen, Europhys. Lett. **28**, 335 (1994).
[20] B. Baumeier, P. Kruger, and J. Pollmann, Phys. Rev. B **76**, 085407 (2007).
[21] J. Yu, D. Yu, Y. Chen, H. Chen, M. Lin, B. M. Cheng, J. Li, and W. Duan, Chem. Phys. Lett. **476**, 240 (2009).
[22] Z. Zhang, W. Guo, and Y. Dai, Appl. Phys. Lett. **93**, 223108 (2008).
[23] S. Okada, S. Saito, and A. Oshiyama, Phys. Rev. B **65**, 165410 (2002).
[24] Z. Zhang, W. Guo, and Y. Dai, J. Appl. Phys. **105**, 084312 (2009).
[25] X. Zhao, Y. Liu, S. Inoue, T. Suzuki, R. O. Jones, and Y. Ando, Phys. Rev. Lett. **92**, 125502 (2004).
[26] G. Kresse and J. Furthmuller, Phys. Rev. B **54**, 11169 (1996).
[27] M. Terauchi, M. Tanaka, K. Suzuki, A. Ogino, and K. Kimurab, Chem. Phys. Lett. **324**, 359 (2000).
[28] G. Makov and M. C. Payne, Phys. Rev. B **51**, 4014 (1995).
[29] M. Posternak, A. Baldereschi, A. J. Freeman, E. Wimmer, and M. Weinert, Phys. Rev. Lett. **50**, 761 (1983).
[30] E. R. Margine and V. H. Crespi, Phys. Rev. Lett. **96**, 196803 (2006).
[31] X. H. Yan, Y. Xiao, J. W. Ding, Z. H. Guo, Y. R. Yang, and D. L. Wang, Phys. Rev. B **75**, 195442 (2007).
[32] A. G. Souza Filho, V. Meunier, M. Terrones, B. G. Sumpter, E. B. Barros, F. Villalpando-Páez, J. Mendes Filho, Y. A. Kim, H. Muramatsu, T. Hayashi, M. Endo, and M. S. Dresselhaus, Nano Lett. **7**, 2383 (2007).
[33] R. Moradian, S. Azadi, and H. Refii-tabar, J. Phys.: Condens. Matter **19**, 176209 (2007).
[34] X. H. Sun, C. P. Li, W. K. Wong, N. B. Wong, C. S. Lee, S. T. Lee, and B. K. Teo, J. Am. Chem. Soc. **124**, 14464 (2002).
[35] Z. H. Zhang and W. L. Guo, J. Am. Chem. Soc. **131**, 6874 (2009).
[36] Y. H. Kim, K. J. Chang, and S. G. Louie, Phys. Rev. B **63**, 205408 (2001).
[37] X. Bai, D. Golberg, Y. Bando, C. Zhi, C. Tang, M. Mitome, and K. Kurashima, Nano Lett. **7**, 632 (2007).
[38] Y. Kinoshita, S. Hase, and N. Ohno, Phys. Rev. B **80**, 125114 (2009).
[39] Z. Xu, D. Golberg, and Y. Bando, Nano Lett. **9**, 2251 (2009).
[40] J. Cumings, P. G. Collins, and A. Zettl, Nature (London) **406**, 586 (2000).
[41] P. G. Collins, M. S. Arnold, and P. Avouris, Science **292**, 706 (2001).